

**Artificially-Imposed Mushy Zone on an Enthalpy Scheme for Solution of the One  
Dimensional Two-Phase Stefan Problem**

Sherry Linn

Wanzhen Lu

Terrance McCotter

Victoria Vaughn

University of Tennessee, Knoxville

Mathematics Research Experience for Undergraduates

Summer, 2007

Drs. Vasilios Alexiades and Cheng Wang

Faculty Advisors

## Abstract

The two-phase Stefan problem is considered in this article. The mathematical model is introduced and an explicit enthalpy numerical method is discussed and implemented. The numerical and exact solutions are compared using the material properties of Glauber's salt. Moreover, a "mushy 2-phase" method is considered. This scheme modifies the enthalpy-temperature relation by introduction of a narrow "mushy zone" of width  $\kappa$ . The effect of  $\kappa$  is addressed and the two methods are compared.

### 1. Introduction

In this paper, we discuss the two-phase Stefan problem in one dimension, which is the classical model for phase-change processes, such as melting and solidification. The mathematical model and the exact Neumann solution to a special case are presented.

We then look at an explicit enthalpy scheme to solve all cases of the one-dimensional two-phase Stefan problem. This involves the discretization of space, time, heat balance, flux, and initial and boundary conditions. The numerical results from our explicit enthalpy scheme program are compared to the exact solution. Melt front, temperature history, and temperature profile plots are created to measure the differences between the numerical and exact solution. The overall error decreases as the number of nodes increases.

Finally, we introduce the "mushy 2-phase" scheme, which is based on the enthalpy method but differs in that it has a mushy zone of width  $\kappa$ . We discuss the effect of  $\kappa$  on the accuracy of the solution. Finally, we compare the mushy and enthalpy schemes.

For our numerical experiments, we modified the example of melting a solid piece of sodium sulfate decahydrate, known as Glauber's salt, found in *Mathematical Modeling of Melting and Freezing Processes* [1 pp.55-56].

## 2. The Stefan Problem

The two-phase Stefan problem is a realistic problem to model melting and freezing processes. A certain phase change material (PCM) can be initially solid or liquid. The problem is covered in detail in Alexiades and Solomon's book [1]. For ease in computing, we look at melting processes only. Consider a PCM, initially solid at temperature  $T_s$ , below (or equal to) the melting temperature,  $T_m$ . Melting is induced by imposing a constant temperature that is greater than the melting temperature at the left boundary  $x = 0$ . It should be noted that "two phase" refers to the two phases present in the process: the solid being heated to melting point and the resulting liquid being heated up towards the higher temperature imposed at  $x = 0$ .

In order to formulate the Stefan problem, it is necessary to make certain assumptions about the substance being melted and the physical processes taking place. The first assumption is that the PCM retains a constant density while undergoing phase change at a fixed melting temperature. Hence, we assume that the density of the PCM as a solid is equal to its density as a liquid. We also assume that heat is isotropically transferred by conduction only, not convection. Furthermore, the latent heat is assumed constant, and it is only released at the phase-change temperature.

The specific heats,  $c_p^S$  and  $c_p^L$ , and thermal conductivities,  $k_S$  and  $k_L$ , are also assumed to be constants, though different for solid and liquid. The interface, an unknown characteristic of

the phase change model, is considered sharp (i.e., having zero thickness). Finally, the effects of supercooling and surface tension at the interface are assumed to be insignificant.

The quantities involved in heat conduction are temperature  $T$ , enthalpy  $e$ , and heat flux  $q$ . The phases can be characterized by either temperature or energy. The PCM is solid when  $e < 0$  and liquid when  $e > L$ , where  $L$  is the latent heat. Equivalently, if  $\psi$  is the density and  $E = \psi e$  is the energy per unit volume, the PCM is solid when  $E < 0$  and liquid when  $E > \psi L$ . At  $T = T_m$ , the enthalpy  $E$  undergoes a jump equal to the latent heat  $\psi L$ . This occurs at the mushy zone region.

The heat flux, which is the amount of heat crossing a unit area per unit time, is given by Fourier's Law:  $q = -k \nabla T$ . The heat absorbed by the PCM is related to its temperature by  $de = c dT$ . Substituting these two equations into the energy conservation law—

$(\psi e)_t + \text{div}(\vec{q}) = F$ , where  $F$  is any internal source of energy—yields the heat equation

$T_t = \zeta \nabla^2 T + F$ , where  $\zeta = \frac{k}{\psi c_p}$ . In one space dimension, given no internal sources, we have

$T_t = \zeta T_{xx}$ . Because the Stefan problem has an exact solution only when dealing with a slab of PCM of semi-infinite length, i.e.,  $x \in [0, \infty)$  for space along the  $x$ -axis, we will concern ourselves with that case. The two-phase problem can then be expressed as follows below.

Heat Equations in Melt and Solid Regions:

$$\begin{aligned} T_t &= \zeta_L T_{xx}, 0 \leq x \leq X(t), t \geq 0 & \zeta_L &= \frac{k_L}{\psi c_p^L} \\ T_t &= \zeta_S T_{xx}, X(t) \leq x, t \geq 0 & \zeta_S &= \frac{k_S}{\psi c_p^S} \end{aligned}$$

Interface temperature:

$$T(X(t), t) = T_m, \quad t \geq 0$$

Stefan condition:

$$\rho L X'(t) = 4k_L T_x(X(t), t) - 2k_S T_x(X(t), t) = 0.$$

Initial conditions:

$$T(x, 0) = T_S \quad \{ T_m, \quad x \} 0, X(0) = 0$$

Boundary conditions:

$$T(0, t) = T_L \quad \{ T_m, \quad t \} 0 \\ 4k_S T_x(l, t) = 0,$$

The general Stefan problem is derived in the book [1 p. 47].

### 3. The Neumann Solution

For the semi-infinite slab starting at  $x = 0$ , an explicit solution can be found for the two-phase Stefan problem in terms of the similarity variable  $\zeta = \frac{x}{\sqrt{t}}$  [1 p. 47]. Called the Neumann

solution, it turns out to be the following:

$$\text{Interface location: } X(t) = 2\zeta\sqrt{\zeta_L t}, \quad t > 0$$

Temperature in the liquid region  $0 < x < X(t), t > 0$ :

$$T(x, t) = T_L + (T_L - T_m) \frac{\text{erf}\left(\frac{x}{2\sqrt{\zeta_L t}}\right)}{\text{erf}(\zeta)}$$

Temperature in the solid region  $x > X(t), t > 0$ :

$$T(x, t) = T_S + 2(T_m - T_S) \frac{\text{erf}\left(\frac{x}{2\sqrt{\zeta_S t}}\right)}{\text{erfc}(\zeta\sqrt{\zeta_L / \zeta_S})},$$

where the constant  $\zeta$  is determined as a root of the transcendental equation

$$\zeta\sqrt{\phi} = \frac{St_L}{\exp(\zeta^2) \operatorname{erfc}(\zeta)} - 4 \frac{St_L}{\exp(\zeta^2) \frac{\zeta_L}{\zeta_s} \operatorname{erfc}(\zeta \sqrt{\frac{\zeta_L}{\zeta_s}})}$$

where  $St_L = \frac{c_L(T_L - T_m)}{L}$  and  $St_s = \frac{c_s(T_m - T_s)}{L}$  are the two Stefan numbers. It has been shown as

an exercise [1 p.57 Problem 5] that the function

$$f(\zeta) = \frac{St_L}{\exp(\zeta^2) \operatorname{erfc}(\zeta)} - 4 \frac{St_L}{\exp(\zeta^2) \frac{\zeta_L}{\zeta_s} \operatorname{erfc}(\zeta \sqrt{\frac{\zeta_L}{\zeta_s}})}$$

is strictly decreasing and thus intersects the line  $\zeta\sqrt{\phi}$  at exactly one positive root  $\zeta$ .

#### 4. The Enthalpy Scheme

A numerical scheme, based on the discretization of the energy conservation law

$E_t + 2q_x = 0$ , to solve the Stefan problem with any acceptable boundary conditions is discussed in [1].

Let  $\Delta x_j$  = length of  $j$ th subinterval, containing the node  $x_j$ , the endpoints of the  $j$ th subinterval are  $x_{j+1/2} = x_j + \frac{\Delta x_j}{2}$  and  $x_{j-1/2} = x_j - \frac{\Delta x_j}{2}$ ,  $j = 1, \dots, M$ , with  $x_{1/2} = 0, x_{M+1/2} = l$ . For uniform partition, the points become  $x_{1/2} = 0, x_{j+1/2} = (j+1)\Delta x, j = 1, \dots, M$  and  $x_{M+1/2} = M\Delta x = l$ . For  $\Delta t_n = \Delta t$  and all  $n$ , we have:  $t_n = n\Delta t, n = 0, 1, 2, \dots$

The exact solution  $T(x,t)$  is denoted as before, and  $T(x_j, t_n)$  represents the temperature value at node  $x_j$  at time  $t_n$ , the numerical approximation is given by  $T_j^n = T(x_j, t_n)$ .

Subsequently, we need to discretize the heat balance:  $E_t + 2q_x = 0$ , in which

$$E = \int_{T_{ref}}^T \rho c(T) dT - \rho c [T - T_{ref}] = \text{thermal energy per unit volume, and } q = -k \frac{\partial T}{\partial x} = \text{heat flux}$$

(Fourier's law). The explicit scheme can be written as  $E_j^{n+1} = E_j^n + \frac{\Delta t_n}{\Delta x_j} [q_{j+1/2}^n - q_{j-1/2}^n]$ . Moreover,

the discretization of the flux and the heat equation becomes  $q = -k \frac{\partial T}{\partial x} = -4k \frac{\Delta T}{\Delta x}$  (Fourier's Law).

Another important step is the implementation of the boundary condition at each time  $t_n$ .

The boundary flux can be written as:  $q_{1/2}^n = -4 \frac{T_1^n - T_0^n}{R_{1/2}}$ , with  $R_{1/2} = \frac{\Delta x_1}{k_1}$ . With the above

discretizations, we are ready to present this scheme:

Initial value:

$$T_j^0 = T_{init}(x_j), \text{ for } j = 1, \dots, M$$

Boundary conditions:

$$T_0^n = T_a, \text{ temperature at left boundary.}$$

$$T_M^n = T_b, \text{ temperature at right boundary.}$$

Keep in mind that we can impose any boundary condition at  $x = 1$ . When we later run the code and compare it to the exact solution, we impose  $T_b^n = T(x_n, t_{n+1})$ .

$$\text{Interior Values: } T_j^{n+1} = T_j^n + \frac{\Delta t_n}{\Delta x_j} \left[ -4 \frac{T_j^n - T_{j+1/2}^n}{R_{j+1/2}} + 4 \frac{T_j^n - T_{j-1/2}^n}{R_{j-1/2}} \right], \text{ for } j = 1, \dots, M$$

$$\text{where } q_{j+1/2}^n = -4 \frac{T_j^n - T_{j+1}^n}{R_{j+1/2}} \text{ with } R_{j+1/2} = \frac{\Delta x_{j+1}}{k_{j+1}} + \frac{\Delta x_j}{k_j} \text{ for } j = 1, \dots, M.$$

The enthalpy and temperature relation can be written as

$$E = \begin{cases} \rho c_s [T - T_m], & T \leq T_m \text{ (solid)} \\ \rho c_L [T - T_m] + \rho L, & T > T_m \text{ (liquid)} \end{cases};$$

therefore,  $T$  can be presented as:

$$T \mid \begin{cases} T_m - 2 \frac{E}{\psi c_s}, & E \geq 0 \quad (\text{solid}) \\ T_m, & 0 \leq E \leq \psi L \quad (\text{interface}) \\ T_m - 2 \frac{E - 4 \psi L}{\psi c_L}, & E \geq \psi L \quad (\text{liquid}) \end{cases}$$

We initialized the temperature and enthalpy:  $T_j^0 \mid T_{init}(x_j)$ ,  $j \mid 1, 2, \dots, M$ ,  $E_j^0$ ,  $j \mid 1, 2, \dots, M$ , respectively. Since resistances and fluxes were the major force to update enthalpies, we computed these quantities as follows:

$$R_{j41/2} \mid \frac{\Delta x_{j41}}{2k_{j41}} - 2 \frac{\Delta x_j}{2k_j} \quad \text{and} \quad q_{j41/2} \mid 4 \frac{T_j - 4T_{j41}}{R_{j41/2}}, \quad j \mid 2, \dots, M.$$

Now we are able to update the temperature and the liquid fraction as the following:

$$T_j^n \mid \begin{cases} T_m - 2 \frac{E_j^n}{\psi c_s}, & E_j^n \geq 0 \quad (\text{solid}) \\ T_m, & 0 \leq E_j^n \leq \psi L \quad (\text{interface}) \\ T_m - 2 \frac{E_j^n - 4 \psi L}{\psi c_L}, & E_j^n \geq \psi L \quad (\text{liquid}) \end{cases}$$

$$\text{and} \quad \zeta_j^n \mid \begin{cases} 0, & \text{if } E_j^n \geq 0 \quad (\text{solid}) \\ \frac{E_j^n}{\psi L}, & \text{if } 0 \leq E_j^n \leq \psi L \quad (\text{mushy}) \\ 1, & \text{if } \psi L \leq E_j^n \quad (\text{liquid}) \end{cases}$$

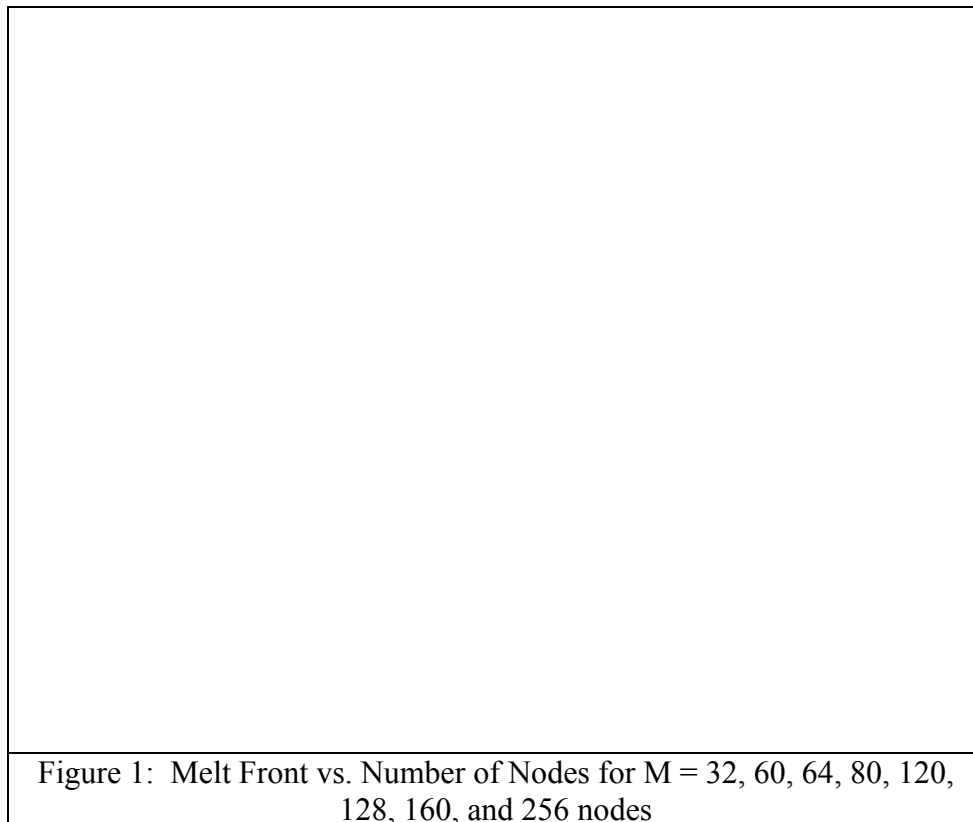
Once the temperature is determined, the enthalpy  $E_j^{n21}$  can be updated at the next time step  $t_{n21}$ . An additional required condition is the Courant-Friedrichs-Lewy (CFL) condition

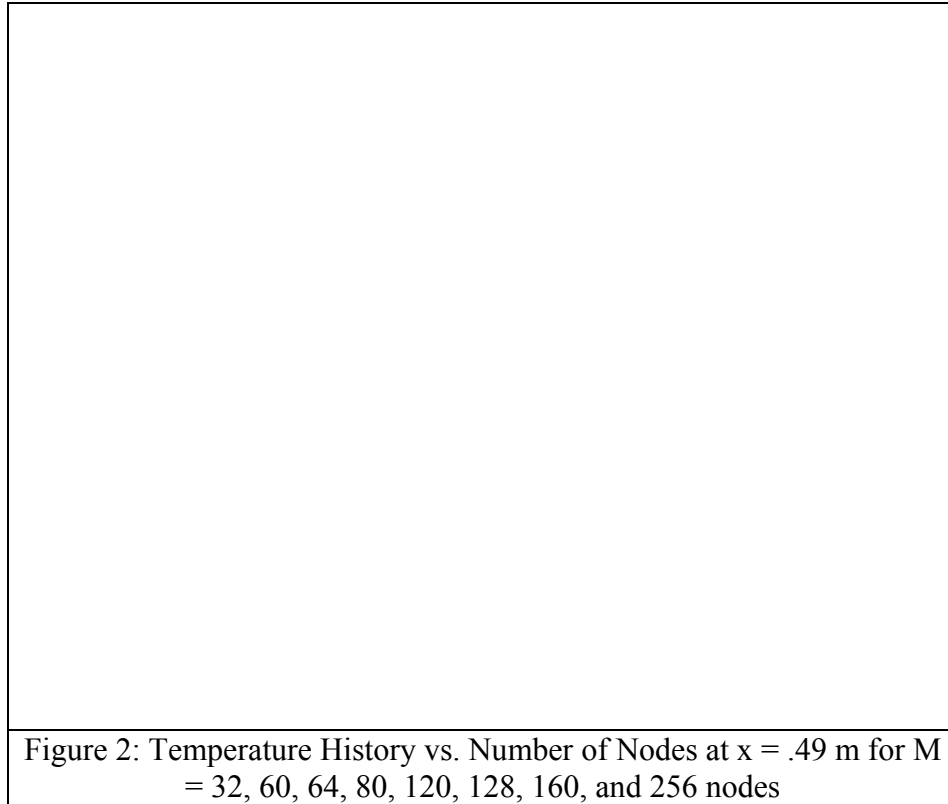
which states that  $\Delta t \leq \frac{\Delta x^2}{2\zeta}$  in order “to ensure numeric stability” [1 pg. 195].

## 5. Error Analysis of Stefan2p program

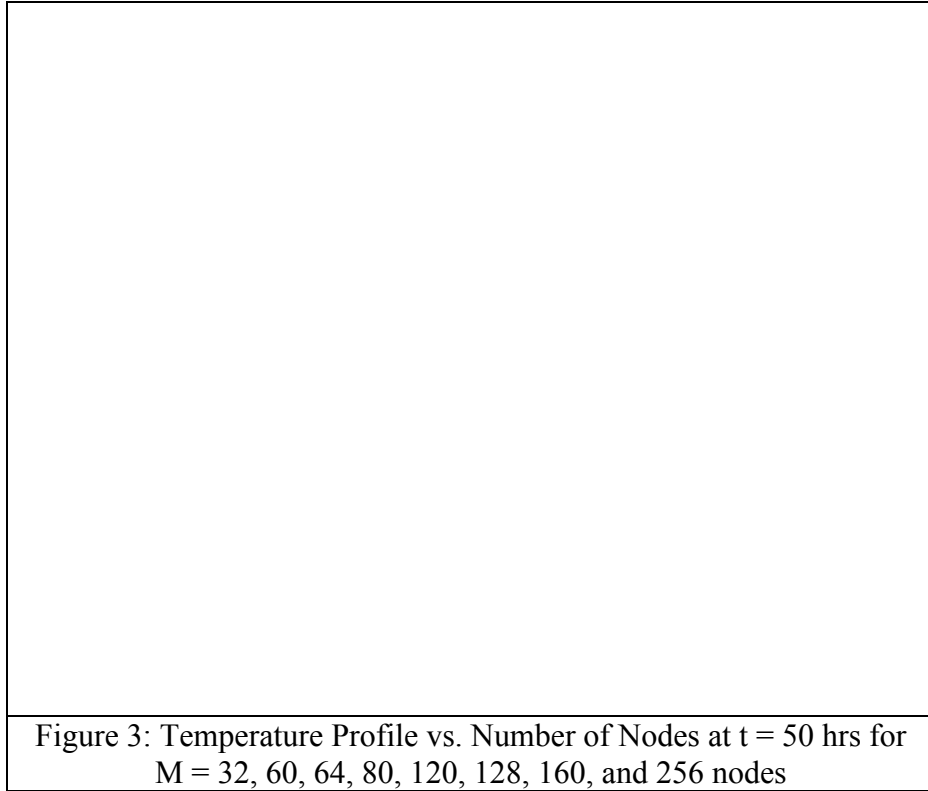
Using Matlab, we coded this scheme as a program that we will refer to as stefan2p. As noted before, all the following results come from running the program with the boundary conditions and material properties from Alexiades' Glauber's salt example [1 pp.55-56] with  $x \in [0,1]$ . We looked at the maximum error in all cases.

When we ran the stefan2p program for 32, 60, 64, 80, 120, 128, 160, and 256 nodes, fixing all other input variables, we found that the general trend was a decrease in error as the number of nodes increased. The error for 60 nodes was smaller than that for 64 nodes by 0.000391. This is the only occurrence of an increase in error with an increase in number of nodes in the graph of the max error of the front. (See Figure 1.) We found that the error in the temperature history (at  $x \approx 0.49$  m) decreased monotonically as the number of nodes increased. Figure 2 is a graph of these errors.





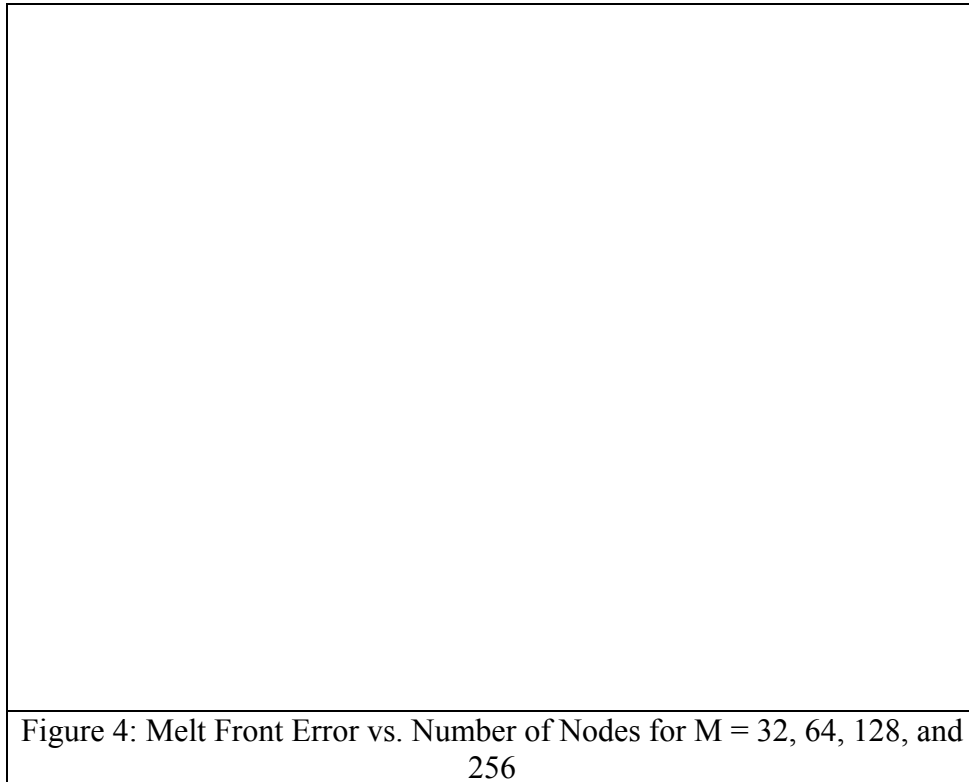
In the graph of the max error of the temperature profile (at  $t = 180,000$  sec. = 50 hrs.) versus the number of nodes, we found that the general trend was a decrease in error as the number of nodes increased. However, the error does not decrease monotonically, as Figure 3 illustrates. For example, the error from 60 to 64 nodes increased by 0.540901. (See the first two columns of Chart 1.)



<b>CHART 1</b>		
Max errors for numeric schemes at various numbers of nodes: Melt front X(t). For mushy2p, $\kappa = 1/M$ .		
M	stefan2p	mushy2p
32	0.00924214308408	0.00923587718350
40	0.00863849122976	0.00863315374731
60	0.00407108310372	0.00406620001060
64	0.00446192843668	0.00445658439565
80	0.00303255235793	0.00302570724513
120	0.00202170157196	0.00201865879723
128	0.00167033322433	0.00165883739437
160	0.00139349859310	0.00138860185728
240	0.00101085078598	0.00101008996667
256	0.00083515988731	0.00083228440722

We then considered only binary values for M. When we run the program for 32, 64, 128, and 256 nodes, fixing all other input variables, the results show that the melt front max error decreased monotonically as the number of nodes in the mesh increased. (See Figure 4.) We also

find this to be the case for the temperature history (at  $x \approx 0.49$  m) and the temperature profile (at  $t = 50$  hrs) as shown in Chart 1 (first two columns) and Figures 5 and 6.



<b>CHART 1</b>		
Max errors for numeric schemes at various numbers of nodes: Melt front $X(t)$ . For mushy2p, $\kappa = 1/M$ .		
M	stefan2p	mushy2p
32	0.00924214308408	0.00923587718350
40	0.00863849122976	0.00863315374731
60	0.00407108310372	0.00406620001060
64	0.00446192843668	0.00445658439565
80	0.00303255235793	0.00302570724513
120	0.00202170157196	0.00201865879723
128	0.00167033322433	0.00165883739437
160	0.00139349859310	0.00138860185728
240	0.00101085078598	0.00101008996667
256	0.00083515988731	0.00083228440722

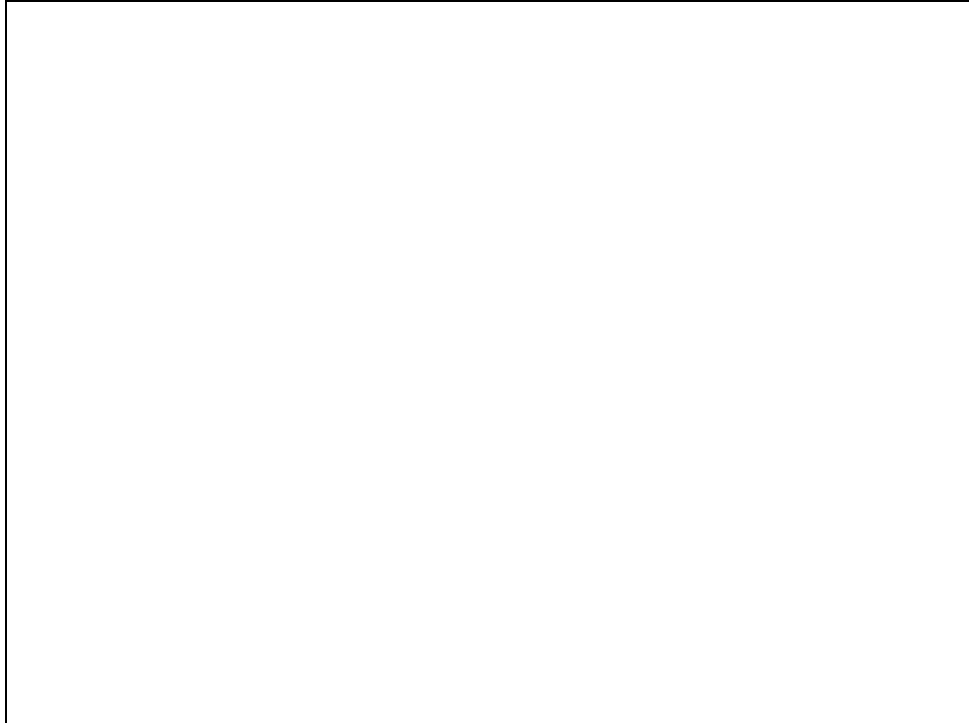


Figure 5: Temperature History Error vs. Number of Nodes at  $x = .49$  m for  $M = 32, 64, 128, 256$

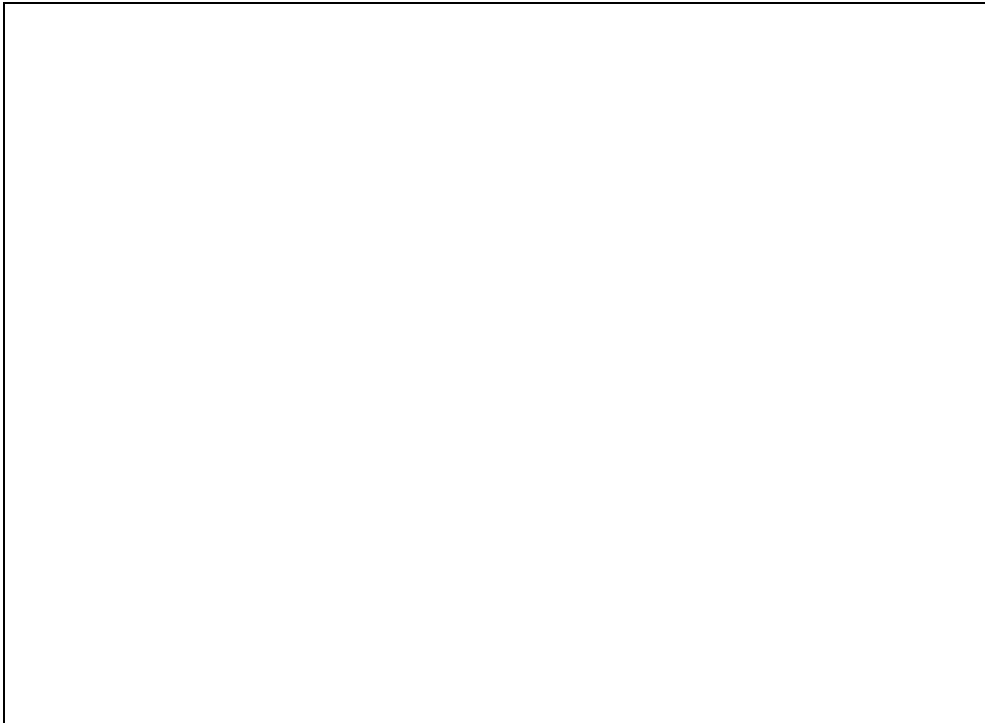


Figure 6: Temperature Profile Error vs. Number of Nodes at  $t = 50$  hrs for  $M = 32, 64, 128, 256$

Note that the errors for the temperature histories are not at exactly the same position along the slab. This is because the temperature for the numerical scheme must be measured at a node on the mesh. As the number of nodes changes, the position of each node changes. Because of the assumption that the distance between the internal nodes of the mesh is constant, it would be difficult or even impossible in some cases to choose an ending point and a corresponding node number so that the node fell directly on a certain location along the slab. To easily evaluate at similar  $x$ -values, one can take the number of temperature values calculated in the numerical scheme, divide by a natural number, and round down to a whole number. In the case of the Glauber's salt example, we used the  $i$ th node, where  $i$  is the integer part of  $(M+2)/2$ , resulting in positions close to  $x = 0.49$  m.

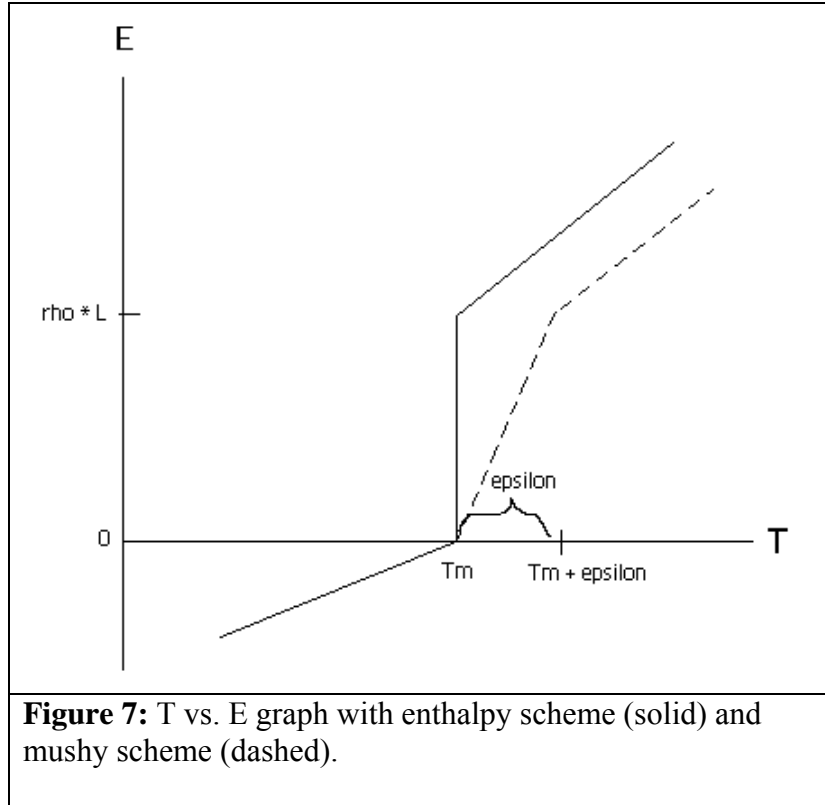
There were some anomalies in our numerical results when we ran `stefan2p` with certain combinations of input variables. One such occurrence was in the temperature histories. When we ran `stefan2p` with  $x = 0.32$  m,  $t_{\max} = 360,000$  sec, and  $M = 40$ , we found that the temperature started to decrease for the last six of 100 output times even though there was no change in the imposed melting temperature (Chart 2).

Chart 2		
Max error for temperature T(x,t) history at x = 3.125e-1 from stefan2p.		
time	T numeric	T exact
3.884884E+03	2.500000E+01	2.500099E+01
7.416597E+03	2.502876E+01	2.504612E+01
1.094831E+04	2.517255E+01	2.519102E+01
1.448002E+04	2.538946E+01	2.540609E+01
1.801174E+04	2.561837E+01	2.565172E+01
2.189662E+04	2.588868E+01	2.592890E+01
2.542833E+04	2.614807E+01	2.617438E+01
...	...	...
3.277430E+05	3.101303E+01	3.105469E+01
3.312747E+05	3.101513E+01	3.106946E+01
3.348064E+05	3.101656E+01	3.108402E+01
3.386913E+05	3.101750E+01	3.109977E+01
3.422230E+05	3.101785E+01	3.111388E+01
3.457547E+05	3.101781E+01	3.112778E+01
3.492864E+05	3.101743E+01	3.114148E+01
3.528181E+05	3.101675E+01	3.115499E+01
3.567030E+05	3.101572E+01	3.116963E+01
3.602347E+05	3.101455E+01	3.118274E+01

Another abnormality in our results were the fluctuations in the max error of the temperature profile discussed above. One possible explanation for this is the mixing of binary and non-binary numbers of nodes since additional error is more likely to occur with non-binary numbers due to the computer arithmetic used in the numerical computations.

## 6. The “Mushy” Scheme

The main purpose of this project is to look at a variation of the enthalpy method in which the temperature vs. enthalpy curve is differentiable in the mushy region. This is achieved by forcing a mushy zone of predetermined length  $\kappa$  on the model. Figure 7 illustrates this with a graph of temperature T vs. enthalpy E. We call this scheme and program mushy or mushy2p. The explicit scheme was chosen for ease and expediency. The code for the new scheme is compared side-by-side to the enthalpy scheme code in Chart 3.



<b>CHART 3</b>	
Excerpt from mushy2p code ("mushy" scheme)	Excerpt from stefan2p code (enthalpy scheme)
<pre> T(1) = Ta; %Boundary condition.  for i=1:M   if E(i) &lt;= 0.0 %Solid.     T(i+1) = Tm + E(i)/rho/cpS;     lq(i) = 0.0;   elseif E(i) &lt; rho*Lat %Mushy zone.     T(i+1) = Tm + E(i)*epsilon/rho/Lat;     lq(i) = (T(i+1) - Tm)/epsilon;     Frontn = xf(i) + lq(i).*Dx;   else %E(i) &gt;= rho*Lat %Liquid.     T(i+1) = Tm + (E(i) - rho*Lat)/rho/cpL;     lq(i) = 1.0;   end end T(M+2) = Tb; %Boundary condition. </pre>	<pre> T(1) = Ta; %Boundary condition.  for i=1:M   if E(i) &lt;= 0 %Solid.     lq(i) = 0;     T(i+1) = Tm + E(i)/rho/cpS;   elseif E(i) &lt; rho*Lat %Mushy zone.     lq(i) = E(i)/rho/Lat;     T(i+1) = Tm;     Frontn = xf(i) + lq(i).*Dx;   else %E(i) &gt;= rho*Lat %Liquid.     lq(i) = 1;     T(i+1) = Tm + (E(i) - rho*Lat)/rho/cpL;   end end T(M+2) = Tb; %Boundary condition. </pre>

From Figure 7, the T vs. E curve is taken to be linear for  $T \in [T_m, T_m + \kappa]$ , i.e.,  $E \in (0, \psi L)$ .

Hence, in that region we get the following equation:

$$T_i^{n21} = T_m + 2 E_i^{n21} \left( \frac{\kappa}{\psi L} \right)$$

The liquid fraction at that mushy zone control volumes is then taken to be  $lq_i^{n21} = T_i^{n21} - T_m \left( \frac{1}{\kappa} \right)$ .

The two aspects to be understood about the mushy scheme are the effect of the imposed  $\kappa$  on the enthalpy scheme and the accuracy of this new scheme compared to that of the original enthalpy scheme. We experimented with the same parameters as before and compared the mushy2p temperatures to the exact solution.

First, the errors in mushy2p, given different values of  $\kappa$ , were compared. The input parameters include  $\Delta t = 0.98 \left( \frac{\Delta x^2}{\psi c_p L} \right)$  and  $t_{\max} = 180,000 \text{ sec.} = 50 \text{ hrs.}$  The numbers of control

volumes (M) used were 64 and 128. For the mushy zone, we chose  $\kappa = C \left( \frac{\Delta x}{\Delta t} \right)$  for

$C = \frac{3}{2}, \frac{5}{4}, 1, \frac{3}{4}, \frac{1}{2}, \frac{1}{4}, \frac{1}{8}$ . As can be seen from Charts 4, 5, and 6, the maximum error for

temperature history and profile and for the interface all increase steadily, though slowly proportionally, as  $\kappa$  decreases.

<b>CHART 4</b>				
Error in melt front location X(t) from mushy2p.				
	M = 64.		M = 128.	
C	$\kappa = C/M$	max error	$\kappa = 1/M$	max error
1.500	0.023437500	0.00445391329551	0.0117187500	0.00165307783498
1.250	0.019531250	0.00445524876889	0.0097656250	0.00165595852401
1.000	0.015625000	0.00445658439565	0.0078125000	0.00165883739437
0.750	0.011718750	0.00445792017579	0.0058593750	0.00166171307921
0.500	0.007812500	0.00445925610933	0.0039062500	0.00166458211765
0.250	0.003906250	0.00446059219628	0.0019531250	0.00166745440697
0.125	0.001953125	0.00446126029728	0.0009765625	0.00166889394234

<b>CHART 5</b>				
Error in temperature T(x,t) history at x = x <sub>1</sub> from mushy2p.				
	M = 64. x <sub>1</sub> = 0.4921875 m		M = 128. x <sub>1</sub> = 0.49609375 m	
C	κ = C/M	max error	κ = 1/M	max error
1.500	0.023437500	0.03250661391631	0.0117187500	0.01842168143398
1.250	0.019531250	0.03313961267450	0.0097656250	0.01877977515984
1.000	0.015625000	0.03377520046359	0.0078125000	0.01913684030466
0.750	0.011718750	0.03441253812594	0.0058593750	0.01949511347319
0.500	0.007812500	0.03505729453202	0.0039062500	0.01985459051722
0.250	0.003906250	0.03570260909501	0.0019531250	0.02021469519763
0.125	0.001953125	0.03602547588698	0.0009765625	0.02039513023100

<b>CHART 6</b>				
Error in temperature T(x,t) profile at t = 180,000 sec. = 50 hrs. from mushy2p.				
	M = 64.		M = 128.	
C	κ = C/M	max error	κ = 1/M	max error
1.500	0.023437500	0.82672317516955	0.0117187500	0.63507037164300
1.250	0.019531250	0.82817918444599	0.0097656250	0.63696326134434
1.000	0.015625000	0.82963045129535	0.0078125000	0.63885783836963
0.750	0.011718750	0.83104935832838	0.0058593750	0.64075407486312
0.500	0.007812500	0.83248031567317	0.0039062500	0.64265197328330
0.250	0.003906250	0.83391207970860	0.0019531250	0.64455153538677
0.125	0.001953125	0.83462826468995	0.0009765625	0.64550194133526

Next, the accuracy of mushy2p is compared to that of stefan2p. We used the same inputs as above, except that we set  $\kappa \propto \frac{1}{M}$  and varied M. Looking at the error in the interface curve, Chart 1, the reader can see that as M increases the mushy2p error decreases; furthermore, the mushy2p errors are consistently smaller, though close, to the stefan2p errors for

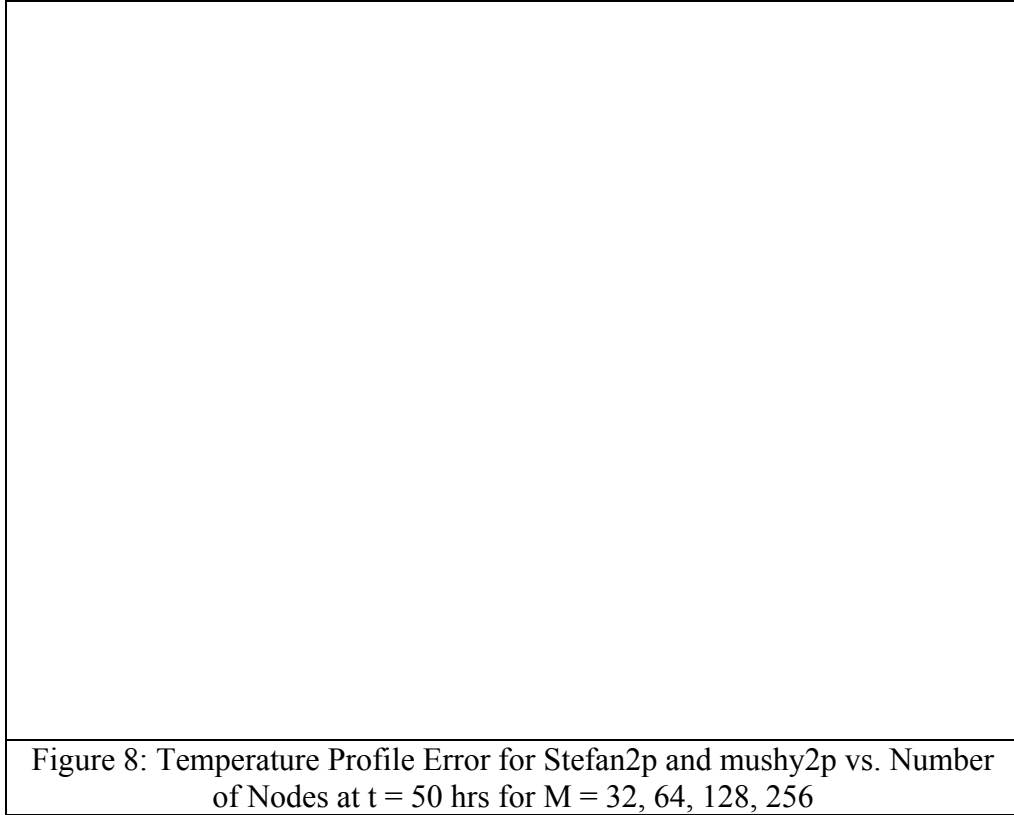
$$\kappa \propto \frac{1}{M}.$$

The temperature history results, taken about halfway through the substance, are similar. Chart 7 shows smaller error with more control volumes. However, for this  $\kappa$ , the mushy2p errors are even smaller than that from stefan2p.

<b>CHART 7</b>			
Max errors for numeric schemes at various numbers of nodes: Max error in temperature $T(x,t)$ history at $x_1$ . For mushy2p, $\kappa = 1/M$ .			
M	$x_1$	stefan2p	mushy2p
32	0.484375000000	0.08163807873548	0.07554693193042
40	0.487500000000	0.06063602835340	0.05612456629782
60	0.491666666700	0.04001984519514	0.03700387382367
64	0.492187500000	0.03634848246029	0.03377520046359
80	0.493750000000	0.03075657297489	0.02846814589175
120	0.495833333300	0.02175548861327	0.02020911411639
128	0.496093750000	0.02057579077834	0.01913684030466
160	0.496875000000	0.01710943502468	0.01594102324600
240	0.497916666700	0.01218277657698	0.01142205789748
256	0.498046875000	0.01153952038154	0.01082570098154

The error in the temperature profile follows the same unsettling lack of monotonicity as that from the stefan2p scheme. The values on Chart 8 show that the mushy errors again follow closely to the stefan2p ones. However, closer study reveals that, for binary values of M, the mushy2p errors are consistently smaller than the stefan2p ones. A plot of these, Figure 8, makes it clearer.

<b>CHART 8</b>		
Max errors for numeric schemes at various numbers of nodes: Temperature $T(x,t)$ profile at $t = 180,000$ sec. = 50 hrs. For mushy2p, $\kappa = 1/M$ .		
M	stefan2p	mushy2p
32	1.39721734740785	1.39111290103978
40	0.65724954768591	0.65923220965860
60	0.29444363002193	0.29550235005397
64	0.83534465188910	0.82963045129535
80	0.14473018624196	0.14560810548880
120	0.22392243999277	0.22044558071511
128	0.64645276473467	0.63885783836963
160	0.40088509319875	0.39523873217349
240	0.19702938327533	0.197151111147884
256	0.12053866446253	0.11876976279872



It is clear that, for  $\kappa \propto \frac{1}{M}$ , the mushy scheme can do better than the original enthalpy scheme. However, further study is needed to discover the optimal value of  $\kappa$  and whether or not the improvement in max error is sufficient to warrant the use of the less physically accurate mushy scheme. The mushy scheme's artificially imposed mushy zone of length  $\kappa$  does not use physical data to better reflect interfaces that are not sharp.

## 7. Conclusion

We introduced the two-phase Stefan problem, run varied experiments, and made comparisons. From the comparison between the Neumann exact and enthalpy numerical solutions, we found that the numerical method can reach the same level of accuracy as the exact solution if the number of nodes,  $M$ , is large enough. In other words, we are able to find the

numerical solution for multi-dimension problems without having to entirely derive the formulation of the Neumann exact solution [1 pg. 199].

We also explored the explicit scheme with  $\kappa$ -long mushy zone. The max error was found to increase as  $\kappa$  decreased, which was unexpected. The optimal value for  $\kappa$  needs to be studied. Additionally, our results showed that mushy2p achieves a higher level of accuracy than Stefan2p for  $\kappa \propto \frac{1}{M}$  (when  $M$  is a power of 2). This implies that the mushy scheme might be a better way to solve the two-phase problem than the enthalpy scheme. Further research is needed to determine whether this is actually the case. Also to be investigated is whether mushy2p could be extended to higher dimensions as Stefan2p can.

## Bibliography

1. Alexiades, V. and Solomon, A. D., 1993, *Mathematical Modeling of Melting and Freezing Processes*, Hemisphere Publ. Co.: Washington DC.